

Threshold diffusion in a tilted washboard potential

To cite this article: G. Costantini and F. Marchesoni 1999 *EPL* **48** 491

View the [article online](#) for updates and enhancements.

You may also like

- [Interplay of flux guiding and Hall effect in Nb films with nanogrooves](#)
O V Dobrovolskiy, M Hanefeld, M Zörb et al.
- [Depinning and nonequilibrium dynamic phases of particle assemblies driven over random and ordered substrates: a review](#)
C Reichardt and C J Olson Reichardt
- [First-principles study of siloxene and germoxene: stable conformations, electronic properties, and defects](#)
Apostolos Atsalakis and Leonidas Tsetseris

Threshold diffusion in a tilted washboard potential

G. COSTANTINI and F. MARCHESONI

*Istituto Nazionale di Fisica della Materia, Università di Camerino
I-62032 Camerino (Macerata), Italy*

(received 26 May 1999; accepted in final form 30 September 1999)

PACS. 05.40–a – Fluctuation phenomena, random processes, noise, and Brownian motion.

PACS. 02.50Ey – Stochastic processes.

PACS. 05.60–k – Transport processes.

Abstract. – We characterize the locked-to-running transition of a Brownian particle in a tilted washboard potential by looking at its transport properties in the vicinity of the transition threshold. At low temperatures the (normal) spatial diffusion of the particle is enhanced as a consequence of the unlocking mechanism; in the overdamped regime an analytic expression is obtained that relates the particle diffusion constant to its mobility; in the underdamped regime an unusually large diffusion constant is revealed through numerical simulation. The latter regime is analyzed in terms of multiple jump statistics.

Forced Brownian motion in one- or two-dimensional periodic potentials provides an archetypal model of transport in condensed phase, notable examples being resistively shunted Josephson junctions [1], superionic conductors [2], plasma accelerators [3], adsorbates on crystal surfaces [4] and polymers diffusing at interfaces [5]. Brownian diffusion in the overdamped regime is by now a fully understood stochastic process, whose application to physical systems can be worked out in great detail [6, 7]. *Low damping* diffusion, instead, accounts for most inertial effects that play a crucial role in real experiments —think of dislocation losses in metals [8], *I-V* characteristics of shunted Josephson junctions [1, 7], dissipation in certain hysteretic systems [9], etc.— and lead to more complicated transport mechanisms, whose description is not completed, yet, despite Risken’s monumental work [6].

In the present letter we aim at characterizing the locked-to-running transition that takes place when a Brownian particle diffusing on a one-dimensional periodic substrate is subjected to a weak tilt, *i.e.* biased by a uniform, macroscopic gradient of the potential or temperature. At low temperatures such a transition results in an abrupt event, accompanied by an excess of noise in the current response or diffusion in the particle delocalization process.

The Brownian motion in a tilted washboard potential is described by the stochastic differential equation (in rescaled units)

$$\ddot{x} = -\gamma\dot{x} - \omega_0^2 \sin x + F + \xi(t), \quad (1)$$

where the force terms on the r.h.s. represent, respectively, a viscous damping with constant γ ,

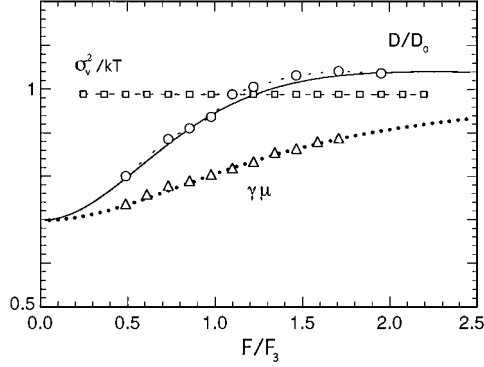


Fig. 1

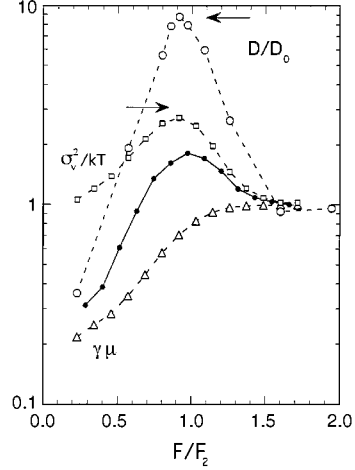


Fig. 2

Fig. 1. – Diffusion in the overdamped regime for different values of the tilt F : $\gamma\mu(F)$, simulation (triangles) and Risken's analytic algorithm (dotted curve); $\sigma_v^2(F)/kT$, simulation (squares); $D(F)/D_0$, simulation (circles) and prediction (6) (solid line) —based on the analytic data for $\gamma\mu(F)$. Parameter values: $\gamma = 100$, $\omega_0 = \pi/4$, $kT/\omega_0^2 = 1.2$ and $F_3 = \omega_0^2$.

Fig. 2. – Diffusion in the underdamped regime for different values of the tilt F : $\gamma\mu(F)$, simulation (triangles); $\sigma_v^2(F)/kT$, simulation (squares); $D(F)/D_0$, simulation (circles) and prediction (6) (solid line) —based on our simulation data for $\gamma\mu(F)$. Parameter values: $\gamma = 10^{-2}$, $\omega_0 = \pi/4$, $kT/\omega_0^2 = 1.2$ and $F_2 = 3.36\gamma\omega_0$. Arrows denote the estimated values of D_m/D_0 (upper) and σ_m^2/kT (lower), respectively.

a spatially periodic, tilted substrate described by the potential

$$V(x, F) = \omega_0^2(1 - \cos x) - Fx, \quad (2)$$

and a stationary Gaussian noise with zero mean $\langle \xi(t) \rangle = 0$ and autocorrelation function $\langle \xi(t)\xi(0) \rangle = 2\gamma kT\delta(t)$.

The time evolution of the stochastic process $x(t)$ is characterized by random switches between a *locked* state with zero average velocity and a *running* state with asymptotic average velocity $\langle v \rangle = \langle \dot{x} \rangle = F/\gamma$. In terms of the mobility $\mu(F) \equiv \langle v \rangle / F$ the locked and running state correspond to $\gamma\mu = 0$ and $\gamma\mu = 1$, respectively. In the noiseless case $\xi(t) \equiv 0$, the average speed of the Brownian particle depends on the initial conditions according to a static hysteresis loop [6]: in the *underdamped* regime $\gamma \ll \omega_0$ the transition from the locked to the running state is triggered by increasing F above $F_3 = \omega_0^2$, while the opposite transition takes place on lowering F below $F_1 = (4/\pi)\gamma\omega_0$. Of course, for sufficiently large values of γ , say, in the *damped* regime with $\gamma > (\pi/4)\omega_0$, the distinction between F_1 and F_3 is meaningless; the locked-to-running transition is located at $F = F_3$, no matter what the initial conditions (fig. 1).

The zero-temperature limit $T = 0+$ brings about a totally different scenario, where the *stationary* dynamics of the underdamped process $x(t)$ is controlled by a single threshold $F_2 \simeq (2 + \sqrt{2})\gamma\omega_0$: At the threshold F_2 the quantity $\gamma\mu(F)$ jumps from zero for $F < F_2$ up to (close to) one for $F > F_2$, stepwise. For finite but low temperatures, $kT \ll \omega_0^2$, the locked-to-running transition is continuous, but still confined within a narrow neighborhood around F_2 (fig. 2). Note that, while the overdamped threshold F_3 corresponds to a static

depinning mechanism, the underdamped threshold F_2 indicates a dynamic transition that may occur even for relatively small tilt values. The curve of the unlocking threshold F_{th} as a function of γ bridges monotonically its asymptotes $F_{\text{th}}(\gamma \rightarrow 0) = F_2$ and $F_{\text{th}}(\gamma \rightarrow \infty) = F_3$, as reported in ref. [6].

The system response is customarily expressed in terms of the probability current $j = \langle v \rangle$, *i.e.* a stationary observable that may be averaged over time according to the ergodic hypothesis [6, 7]. In the present investigation we pursued an alternative approach: We focused on the spatial dispersion of the Brownian particle $x(t)$ along the inclined periodic substrate (2). As the particle runs with average speed $\langle v \rangle$ in the direction of the external force F , the random switches between locked and running state are expected to cause an additional diffusion effect on the particle around its average position $\langle x(t) \rangle$ (namely, the center of mass of its probability density function). To this purpose, we computed numerically the *normal* diffusion constant

$$D = \lim_{t \rightarrow \infty} \frac{1}{2t} \langle [x(t) - \langle x(t) \rangle]^2 \rangle = \lim_{t \rightarrow \infty} \frac{1}{2} \frac{d}{dt} \langle [x(t) - \langle x(t) \rangle]^2 \rangle \quad (3)$$

of the transport process (1)-(2) and studied D as a function of the bias F at constant temperature. In figs. 1 and 2 we display our results for D/D_0 in the over- and underdamped regime, respectively. The quantity $D_0 = kT/\gamma$ denotes Einstein's diffusion constant for the free Brownian motion in one dimension. A peak in the curves of D *versus* F is detectable in the vicinity of the transition threshold F_{th} , irrespective of the value of γ . In particular, at low damping $F_{\text{th}} \simeq F_2$ and the peak of D at $F = F_2$ is very pronounced; at high damping $F_{\text{th}} \simeq F_3$ and the corresponding diffusion peak results in just a bump.

The F -dependence of the diffusion constant in the overdamped regime $\gamma \gg \omega_0$ can be interpreted analytically in the framework of the linear response theory. On extending the approach developed by Risken for the zero-bias case, one derives the following two equalities:

$$D = \lim_{t \rightarrow \infty} \int_0^t \langle \delta v(t) \delta v(t - \tau) \rangle d\tau \quad (4)$$

(see ref. [6], sect. 11.7.1), and

$$\langle v(F + \Delta F) \rangle - \langle v(F) \rangle = \frac{\Delta F}{kT} \int_0^\infty \langle \delta v(t) \delta v(0) \rangle dt \quad (5)$$

(see ref. [6], sect. 7.2), where $\delta v(t) = v(t) - \langle v \rangle$ and ΔF denotes an infinitesimal increment of F . On comparing eqs. (4) and (5), one concludes that

$$\frac{D}{D_0} = \gamma \frac{d\langle v(F) \rangle}{dF} = \gamma \mu(F) + F \frac{d}{dF} [\gamma \mu(F)]. \quad (6)$$

The bump in the $D(F)$ curve of fig. 1 is thus related to the jump of $\mu(F)$ at the threshold $F_{\text{th}} \simeq F_3$. As shown in fig. 2, our prediction (6) does not apply to the underdamped regime, where it grossly underestimates the excess diffusion that accompanies the locked-to-running transition. The reason is simple: eq. (6) has been derived under the assumption that the probability density $P(x, v)$ for the process (1)-(2) factorizes into the product of a Boltzmann distribution for the spatial coordinate $P(x) \sim \exp[-V(x, F)/kT]$ and a Gaussian distribution for the velocity $P(v) \sim \exp[-(v - \langle v \rangle)^2/2kT]$. This is correct in the Smoluchowski limit $\gamma \rightarrow \infty$, whereas for vanishingly small damping values, the transition threshold is characterized by a bimodal distribution of the velocity with peaks at $v = 0$ and $v = F/\gamma$ [6], respectively. The simulation results reported in fig. 1 compare well with prediction (6) within the accuracy of our numerical code.

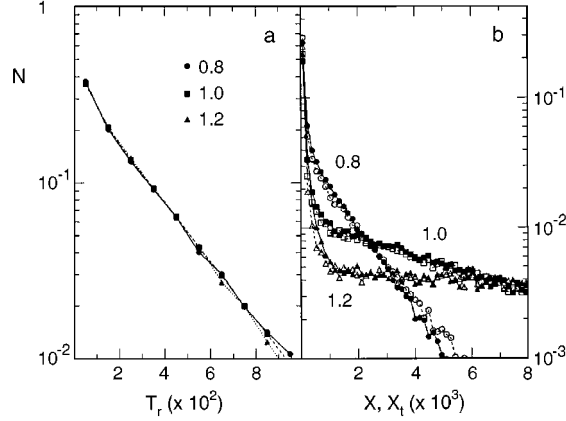


Fig. 3. – Jump statistics in the underdamped regime: (a) $N(T_r)$; (b) $N(X)$ (open markers) and $N(X_t)$ (solid markers) for three values of F/F_2 in the vicinity of the transition threshold. Other simulation parameter values are as in fig. 2. Exponential distributions fit well the simulation data for: $\bar{T}_x = 379$ and $\bar{T}_r = 340$ for $F/F_2 = 0.8$, $\bar{T}_x = 1431$ and $\bar{T}_r = 336$ for $F/F_2 = 1.0$, $\bar{T}_x = 5311$ and $\bar{T}_r = 332$ for $F/F_2 = 1.2$, respectively (estimated accuracy 10%).

Note that the excess diffusion studied here is a *stationary* phenomenon, in contrast with the mechanism underlying the excess diffusion “oscillations” reported in the recent literature [10,11], where the overdamped Brownian motion in the washboard potential was driven periodically in time (with no static bias). By looking at fig. 6 of ref. [10] and fig. 2a of ref. [11], one is led to conclude that our simulation results are consistent with the zero-frequency limit of both time-modulated diffusion models.

We address now the excess threshold diffusion in the underdamped regime $\gamma \ll \omega_0$ [12]. In order to shed light on the underlying locked-to-running switching mechanism, we computed numerically three types of distributions: i) Distributions $N(T_r)$ of the residence times T_r of the Brownian particle at the bottom of a potential well (fig. 3a). The diffusing particle is deemed as locked around a local minimum of $V(x, F)$ if it sojourns within two adjacent potential barriers for a time interval longer than $(2\gamma)^{-1}$ —the characteristic relaxation time of its energy variable. The particle is counted as exiting the potential well where it has been locked any time it crosses the top of one of its confining barriers. ii) Distributions $N(X)$ of the multiple jump (or flight) length X . It is well known that at low damping the Brownian particle can jump over many a potential barrier prior to being retrapped into another metastable state. The observable X denotes here the distance between two trapping $V(x, F)$ minima where the particle has resided consecutively longer than $(2\gamma)^{-1}$. In fig. 3b the distributions $N(X)$ are plotted only for positive flight lengths, that is for $X > 0$, being the number of backward jumps at the transition negligible (see also fig. 4). iii) Distributions $N(T_x)$ of the flight duration T_x (fig. 3b). For the sake of a comparison, we rescaled T_x into an effective length X_t by multiplying T_x times the asymptotic speed F/γ of the *running* state, that is $X_t = (F/\gamma)T_x$. The two distributions $N(X)$ and $N(X_t)$ in fig. 3b appear to overlap.

Figure 3 allows us to state a few properties of the multiple jump dynamics that takes place in a tilted washboard potential [13-17]. Firstly, for tilt values in the neighborhood and above the threshold F_2 , the flight speed comes close to the asymptotic velocity F/γ [7, 9]. Secondly, the long-time tails of $N(T_r)$ and $N(T_x)$ decay according to exponential laws with decay times \bar{T}_r and \bar{T}_x , respectively. We checked that our results for $F = 0$ (zero-bias

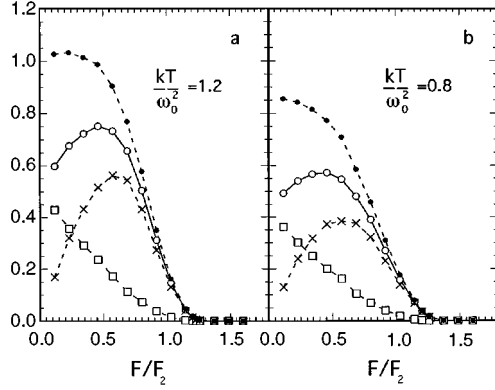


Fig. 4

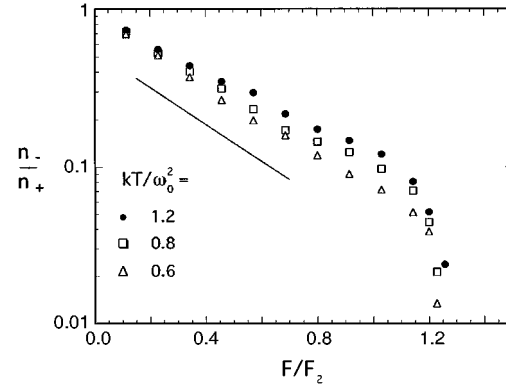


Fig. 5

Fig. 4. – Jump densities in the underdamped regime: $[n_+(F) + n_-(F)]T_0(0)$ (solid circles); $n_+(F)T_0(0)$ (open circles); $[n_+(F) - n_-(F)]T_0(0)$ (crosses); $n_-(F)T_0(0)$ (squares). Parameter values: $\gamma = 10^{-2}$, $\omega_0 = \pi/4$ and $kT/\omega_0^2 = 0.8$ (a), $= 1.2$ (b). The zero-bias escape times are $T_0(0) = 765 \pm 18$ in (a) and $T_0(0) = 361 \pm 15$ in (b).

Fig. 5. – The ratio n_-/n_+ vs. F for the simulation parameters of fig. 4 and $kT/\omega_0^2 = 1.2$ (circles), $= 0.8$ (squares), $= 0.6$ (triangles).

limit) confirm qualitatively the relevant predictions contained in the exhaustive study on the subject published by Bader *et al.* [17]. On the face of the previous remark, the average residence time \overline{T}_r quantifies the permanence of the system in its locked state, with zero speed, whereas \overline{T}_x is to be regarded as the average relocking time of a particle with running flight speed F/γ . Our interpretation of the results of figs. 2 and 3 is verified by the (approximate) self-consistency equation [7]

$$\gamma\mu(F) = \frac{\overline{T}_x}{\overline{T}_r + \overline{T}_x}, \quad (7)$$

which is numerically fulfilled by our simulation for $F \gtrsim F_2$. As F_2 is much smaller than the static threshold F_3 , no surprise that \overline{T}_r , which approximates the average escape time out of a tilted potential well $T_0(F)$ (through either escape paths) [18], decreases weakly with increasing F across the entire transition range. On the contrary, \overline{T}_x increases exponentially with F through the threshold F_2 . The statistics of our distributions $N(T_x)$ is not high enough for us to check Melnikov's predictions for \overline{T}_x [7]. Finally, multiple jumps are particularly frequent at the unlocking transition, only. As a matter of fact, for $F < F_2$ the particle jumps forward by executing a few sparse and relatively short flights; for $F > F_2$ the particle jumps over much longer distances, as the relocking events become rare.

The jump statistics is better illustrated in fig. 4, where the density (namely, the number per unit of time) of forward, n_+ , and backward jumps, n_- , is plotted vs. the bias intensity F . The curve $n_+(F)$ exhibits a broad peak below threshold, due to two competing mechanisms: On applying a very weak external bias $F = 0+$, one causes an asymmetry in the escape process, thus increasing the rate of the jumps in the F direction at the expenses of the number of jumps in the opposite direction; as F approaches the transition range, the length of the forward jumps grows so long that their density falls necessarily to zero. This behavior is reflected by the monotonic decay of $n_-(F)$. As a consistency test, we checked numerically that in the absence of applied bias, $F = 0$, the identity $(n_+ + n_-)T_0 = 1$ holds increasingly well with

decreasing the temperature, as required by the very definition of the escape time T_0 [18].

As anticipated above, the multiple jump dynamics is responsible for the excess spatial dissipation at the locked-to-running transition. The function $D(F)$ attains its maximum D_m at $F \simeq F_2$, almost insensitive to the temperature (see fig. 2). The value of $D_m \simeq D(F_2)$ can be estimated as follows: At the transition the Brownian particle behaves like a random walker with mean velocity $\mu(F_2)F_2$, waiting time \bar{T}_r and average (unidirectional) displacement $(F_2/\gamma)\bar{T}_x$. A standard calculation yields

$$D_m = \left(\frac{F_2}{\gamma}\right)^2 \frac{\bar{T}_x^2}{2\bar{T}_r} [1 - \gamma\mu(F_2)]^2 \simeq \frac{\bar{T}_r}{2} \left(\frac{F_2}{\gamma}\right)^2 [\gamma\mu(F_2)]^2. \quad (8)$$

The r.h.s. equality in eq. (8) was obtained by making use of eq. (7). The actual values of F_2 and $\gamma\mu(F_2)$ can be inferred from the simulation data displayed in fig. 2. Otherwise, F_2 may be given the analytic expression $F_2 \simeq 3.36\gamma\omega_0$ for $T = 0+$ and $\gamma\mu(F_2)$ may be safely approximated to 0.7 for a wide temperature range, say $0.3 < kT/\omega_0^2 < 3.0$, as shown in fig. 11.18 and eq. (11.135) of ref. [6]. Our estimate for D_m is reported in fig. 2 for the reader's convenience.

The multiple jump statistics accounts also for the large variance $\sigma_v^2 = \langle [v - \langle v \rangle]^2 \rangle$ of the particle velocity at the transition threshold. In the overdamped regime the factorization $P(x, v) = P(x)P(v)$ of the probability density implies that in the stationary regime $\langle v \rangle = \mu(F)F$ and $\sigma_v^2 = kT$, no matter what the applied bias. In the underdamped regime the locked-to-running transition amounts to a dynamical *bistable* mechanism with two modes, the locked state $v = 0$ and the running state $v = F_2/\gamma$. On varying the value of F , the bistability of the process is broken and the variance of the random variable $v(t)$ diminishes. Correspondingly, one expects that $\sigma_v^2(F)$ develops a symmetric peak with center at $F \simeq F_2$ and height

$$\sigma_m^2 \simeq \sigma_v^2(F_2) \simeq \gamma\mu(F_2)[1 - \gamma\mu(F_2)] \left(\frac{F_2}{\gamma}\right)^2 + kT. \quad (9)$$

The estimated value of σ_m^2 , too, is reported in fig. 2 and appears to compare well with the results of our simulation.

Finally, we looked at the ratio of backward-to-forward jump density n_-/n_+ as a function of the applied bias. Three curves of n_-/n_+ vs. F at decreasing temperatures are plotted in fig. 5. A further remarkable property of the transition threshold becomes then apparent by inspection: As anticipated above, the density of the backward jumps vanishes monotonically on approaching the transition range; the ratio n_-/n_+ decays according to an exponential law with logarithmic slope only weakly sensitive to the temperature. In view of Risken's activation layer theory, we found a heuristic law for n_-/n_+ vs. F , namely

$$\frac{n_-}{n_+} = \exp \left[-\frac{F}{F_1} \sqrt{\frac{aF_1}{2kT}} \right] \quad (10)$$

with $a = 2\pi$, which seems to fit closely our simulation data [19].

In conclusion, the locked-to-running transition in the underdamped regime is signalled by an excess diffusion of the travelling particle or, equivalently, by an excess noise in the system response. The statistical tools we developed, namely the multiple jump distributions, lend themselves to interesting applications to the escape problem in the limit of zero bias, too. The extension of our method to the symmetric case is matter of ongoing research.

REFERENCES

- [1] BARONE A. and PATERNÓ G., *Physics and Applications of the Josephson Effect* (Wiley, New York) 1982.
- [2] FULDE P., PIETRONERO L., SCHNEIDER W. R. and STRÄSSLER S., *Phys. Rev. Lett.*, **35** (1975) 1776.
- [3] KATSOULEAS T. and DAWSON J., *Phys. Rev. Lett.*, **51** (1983) 392.
- [4] FRENKEN J. W. M. and VAN DER VEEN J. F., *Phys. Rev. Lett.*, **54** (1985) 34; PLUIS B. *et al.*, *Phys. Rev. Lett.*, **59** (1987) 2678; HERSHKOVITZ E., TALKNER P., POLLAK E. and GEORGEVSKII Y., *Surf. Sci.*, **421** (1999) 73.
- [5] NIXON G. I. and SLATER G. W., *Phys. Rev. E*, **53** (1996) 4969.
- [6] RISKEN H., *The Fokker-Planck Equation* (Springer, Berlin) 1984, Chapt. 11.
- [7] MELNIKOV V. I., *Phys. Rep.*, **209** (1991) 1.
- [8] BRAUN O. M., BISHOP A. R. and RÖDER J., *Phys. Rev. Lett.*, **79** (1997) 3692; CATTUTO C. and MARCHESONI F., *Phys. Rev. Lett.*, **79** (1997) 5070.
- [9] BORROMEO M., COSTANTINI G. and MARCHESONI F., *Phys. Rev. Lett.*, **82** (1999) 2820.
- [10] HU GANG, DAFFERTSHOFER A. and HAKEN H., *Phys. Rev. Lett.*, **76** (1996) 4874.
- [11] SCHREIER M., REIMANN P., HÄNGGI P. and POLLAK E., *Europhys. Lett.*, **44** (1998) 416.
- [12] MARCHESONI F., *Phys. Lett. A*, **231** (1997) 61.
- [13] FERRANDO R., SPADACINI R. and TOMMEI G. E., *Phys. Rev. E*, **48** (1993) 2437.
- [14] POLLAK E., BADER J., BERNE B. J. and TALKNER P., *Phys. Rev. Lett.*, **70** (1993) 3299.
- [15] FERRANDO R., SPADACINI R. and TOMMEI G. E., *Phys. Rev. E*, **51** (1995) 126.
- [16] JUNG P. and BERNE B. J., in *New Trends in Kramers' Theory*, edited by P. TALKNER and P. HÄNGGI (Kluwer Academic, Dordrecht) 1995, p. 67.
- [17] BADER J. S., BERNE B. J. and POLLAK E., *J. Chem. Phys.*, **102** (1995) 4037.
- [18] GAMMAITONI L., HÄNGGI P., JUNG P. and MARCHESONI F., *Rev. Mod. Phys.*, **70** (1998) 223.
- [19] BORROMEO M. and MARCHESONI F., to be published.